10-20-2003

Clustering of Galaxies at z ∼ 3 Around the Probable Damped Lyα Absorber Toward QSO APM 08279+5255

Nicolas Bouché
University of Massachusetts Amherst

James D. Lowenthal
Smith College, jlowenth@smith.edu

accepted to ApJ
Preprint typeset using LaTeX style emulateapj v. 11/12/01

CLUSTERING OF GALAXIES AT $Z \sim 3$ AROUND THE PROBABLE DAMPED LY-ALPHA ABSORBER TOWARDS QSO APM 08279+5255

Nicolas Bouché [1,2]
Dept. of Astronomy, University of Massachusetts-Amherst, Amherst, MA 01003 USA;
bouche@astro.umass.edu

James D. Lowenthal [1]
Dept. of Astronomy, Smith College, Northampton, MA 01063 USA; james@earth.ast.smith.edu
accepted to ApJ

ABSTRACT

We present results on the clustering of Lyman break galaxies (LBGs) around a probable damped Lyα absorption (DLA) line cloud at $z_{\rm abs} = 2.974$ from deep $UBVI$ images of the field containing the quasar APM 08279+5255 ($z_{\rm em} = 3.91$). The large area covered by our images, 0.31 deg^2 or $\sim 40 \times 40$ Mpc co-moving at redshift $z = 3$, and their depth, $\mu_{I,\rm AB}(sky) \simeq 27.6$ mag arcsec^{-2}, allow us to identify ~ 450 LBG candidates brighter than $I_{AB} = 24.80$ at $2.75 < z < 3.25$ both close (50 kpc) to the DLA line-of-sight and up to 20 Mpc (co-moving) from the DLA, i.e. physically unrelated. LBG candidates were identified using photometric redshift techniques that include the I magnitude as a prior estimate in addition to the colors. The two are combined using Bayes' theorem. This helps to break the degenerancies that occur in a pure spectral template fitting scheme. The overall rms is $\sigma_z \simeq 0.15$ at $z \sim 3$ based on our analysis of photometric redshifts in the HDF-N.

From the redshift likelihood distributions, we selected LBG galaxies within a redshift slice of width $W_z = 0.15 (\simeq \sigma_z)$ centered on the redshift of the DLA $z_{\rm abs}$.

Within that redshift slice, we find an enhancement of galaxies near the DLA using both the surface density ($\Sigma/\Sigma_g \simeq 3$) and an estimator of the 3-D spatial overdensity ($n/\overline{n}_g \sim 5 \pm 3$). The surface overdensity Σ/Σ_g is significant at the $> 95\%$ significance level on scales $2.5 < r_\theta < 5$ Mpc co-moving. The overdensity can not be related to the QSO environment since the QSO is at $z_{em} = 3.91$. These results imply that some DLA could reside in high density regions.

We search within $45''$ from the line of sight for galaxies responsible for the DLA, and find one candidate with $z_{\rm phot} = 3.03$ that is $26''$ (145 kpc physical) away. From its magnitude $I = 24.65 \pm 0.2$, its luminosity is $M_{I,\rm AB} = -21.35$. Due to its large impact parameter, however, this galaxy is not a likely candidate for the absorber.

Subject headings: galaxies: evolution — galaxies: high-redshift — quasars: absorption lines — quasars: individual (APM08279+5255)

1. INTRODUCTION

Damped Lyα absorbers (DLAs) give rise to the largest neutral hydrogen (HI) column densities ($N_{\rm HI} > 2 \times 10^{20}$ cm^{-2}) of quasar absorption line systems. They are important because they contain the largest reservoir of HI at high redshift, and their detailed nature have been the subject of an ongoing debate. Wolfe et al. (1986) argued that DLAs are massive gas rich disks based on the similarity between the amount of HI contained in DLAs and the stellar masses of disk galaxies today. Later, Wolfe et al. (1995) and Prochaska & Wolfe (1997) argued that DLA kinematics are consistent with those expected from lines of sight intercepting massive rotating thick gaseous disks.

However, theoretical simulations of galaxy formation show that a large range of structures and morphologies can give rise to DLAs (e.g. Katz et al. 1996; Haehnelt, Steinmetz & Rauch 1998; McDonald & Miralda-Escudé 1999). DLAs would arise from the combined effect of a massive central galaxy and/or a number of smaller satellites in a virialized halo (Maller et al. 2000) or filaments (e.g. Haehnelt, Steinmetz & Rauch 1998), i.e., DLAs would lie in over-dense regions.

Several approaches have been used to investigate the nature of high$-z$ DLAs. Broad band imaging surveys of DLAs have been used since Steidel & Dickinson (1992); Steidel & Hamilton (1992) were unsuccessful in finding the absorber, but did find large numbers of Lyman break galaxies (LBGs) (e.g. Steidel & Hamilton 1993). In addition, it has become clear that DLAs (1) show little evolution from $z = 4$ to $z = 1$ in their contribution to the matter density of the Universe $\Omega_{\rm DLA}(z)$ (e.g. Rao & Turnshek 2000; Boissier, Péroux & Pettini 2003, and references therein); (2) show little metallicity evolution (Pettini et al. 1999; Prochaska & Wolfe 2002) from $z = 3$ to $z = 0.3$; (3) have heterogeneous chemical properties (Pettini et al. 2000); (4) have various morphologies (Le Brun et al. 1997; Rao & Turnshek 2000); and (5) have low star formation rates (Kulkarni et al. 2000; Bouché et al. 2001).

These results indicate that DLAs do not participate significantly in the overall chemical enrichment of the Universe and hence do not trace star formation in any straightforward way. Both these observations and theoretical work

[1] Visiting Astronomer, Kitt Peak National Observatory, National Optical Astronomy Observatory, which is operated by the Association of Universities for Research in Astronomy, Inc. (AURA) under cooperative agreement with the National Science Foundation.

[2] EARA Marie-Curie Fellow at the Institute of Astronomy, Cambridge, UK

show that DLAs are not a single type of galaxy, but are merely characteristic of a type of region: namely, one with a large neutral column density (e.g. Khersonsky & Turnshek 1996).

Similarly to broad-band imaging, early attempts to detect diffuse Lyα emission from DLAs at $z > 2$ using deep narrow band imaging (e.g. Lowenthal et al. 1995) did not reveal the absorber, but unveiled a few companion Lyα emitters, hinting at the clustering of galaxies around DLAs. This prompted Wolfe (1993) to calculate the two-point correlation function at $z = 2.6$ and to conclude that indeed Lyα emitters are clustered near DLAs. Some recent Lyα searches succeed in unveiling the absorber (e.g. Fynbo et al. 1999).

Here, we seek to constrain the matter distribution around DLAs at $z \sim 3$ using LBGs as tracers of the large scale structure. Specifically, are the DLAs in *over- or under-dense* regions? Previous attempts at answering this question include the investigation of Gawiser et al. (2001), which ruled out any clustering between galaxies and a DLA at $z \sim 4$. Recently, Adelberger et al. (2003) found only two galaxies within $265''(\sim 5.7h^{-1}$ Mpc) and within $|\Delta z| < 0.0125$ ($\sim 8h^{-1}$ Mpc) of four DLAs at $z \sim 3$ whereas 5.96 were expected. They conclude from the same null hypothesis test used here (see below) that the lack of galaxies near the four DLAs is significant at $> 90\%$ level and argue that this is evidence that DLAs and LBGs 'do not reside in the same parts of the universe'.

In contrast, Francis & Hewett (1993) reported the discovery of super-clustering of sub-DLAs at $z \sim 2.3$. Recent narrow-band imaging (Fynbo et al. 2003, private communication) of the same field shows that spectroscopically confirmed Lyα-emitting galaxies are clustered at the redshift of the two strongest HI clouds. These observations and others (e.g. d'Odorico, Petitjean & Cristiani 2002) show that at least some DLAs reside in overdense regions.

The field of QSO 3C336 shows an over-density of galaxies around an intermediate redshift DLA at $z = 0.656$ (Steidel & Dickinson 1992; Steidel et al. 1997; Bouché et al. 2001). Steidel & Dickinson (1992) suggested the possibility of a cluster at $z = 0.656$. From a sample of spectroscopically confirmed galaxies within $50''$ ($0.4\ h^{-1}$ Mpc co-moving) of the QSO line of sight, Steidel et al. (1997) showed that galaxies are clustered in redshift around the metal-line systems (see Steidel et al. 1997, Fig 7). A closer analysis reveals that they are even more clustered around the DLA: the number of galaxies per unit redshift, dN/dz, peaks at $z = 0.656$ (aside from the peak at $z_{em} = 0.927$). Indeed, out of 11 galaxies at $0.4 < z < 0.85$, four galaxies lie within $\Delta_z < 0.03$ (9,000 km s^{-1}) of the DLA on scales of $\sim 200h^{-1}$ Mpc (co-moving).

In this paper, we present results of our survey of LBGs around a DLA at $z = 2.974$ towards QSO APM 08279+5255. This field is the first of four. The results on the other three (one with some spectroscopy) are still pending and will be presented in Bouché & Lowenthal (2003) along with the details of our procedure and data analysis. Our study is similar to the investigations of Gawiser et al. (2001) and Adelberger et al. (2003); however, our MOSAIC sky coverage is more than 25 times larger, providing us with both extended spatial sensitivity and a built-in control sample of the background surface density of LBGs.

Throughout this paper, we adopt $\Omega_M = 0.3$, $\Omega_\Lambda = 0.7$ and $H_o = 100h$ km s^{-1} Mpc^{-1}; thus, at $z \sim 3$, $1''$ corresponds to $\sim 21.5h^{-1}$ kpc and $1'$ to $\sim 1.29h^{-1}$ Mpc, both *co-moving*. At that redshift, $H(z) \sim 4.46H_o$, so $\delta z = 0.1$ corresponds to $67h^{-1}$ Mpc in co-moving coordinates. Magnitudes are Vega based unless stated otherwise.

2. THE DATA

2.1. *The APM 08279+5255 field*

This field, like the other three in our survey, was selected for the presence of a DLA at $z \sim 3$ and with requirement $z_{abs} \ll z_{em}$. The redshift range $z \sim 3$ is ideal for selecting LBGs efficiently using standard photometric filters.

Even taking into account its gravitational lens magnification $10 - 100\times$, this APM 08279+5255 ranks among the most luminous objects in the Universe (e.g. Irwin et al. 1998; Lewis, Robb & Ibata 1999). The DLA at $z_{abs} = 2.974$ was first reported by Petitjean et al. (2000) based on a high resolution spectrum (6 km s^{-1}) of the QSO APM 08279+5255 ($z_{\rm em} = 3.91$), obtained by Ellison et al. (1999) [3] at the 10-meter Keck telescope with HIRES. Due to uncertainty in the continuum, the DLA's column density is poorly constrained: $19.8 < \log N({\rm HI}) < 20.3$. The absorber could therefore technically be a 'sub-DLA'. However, the Lyα equivalent width $W_{\rm rest}({\rm Ly}\alpha) > 4.8$Å (Petitjean et al. 2000) and its strong MgII equivalent width $W_{\rm rest}({\rm MgII}) > 0.6$Å (Kobayashi et al. 2002) supports its classification as a damped cloud.

Petitjean et al. (2000) estimated a minimum cloud size $r_{\rm DLA} > 200h_{75}^{-1}$ pc from the image separation of the QSO. The most robust estimate is from Tzanavaris & Carswell (2003) who found $r_{\rm DLA} > 450h^{-1}$ pc (assuming the gravitational lens is at $z \sim 1$). The QSO and DLA properties are summarized in Table 1.

2.2. *Observations, data reduction & completeness*

The observations, summarized in Table 2, were carried out with the MOSAIC camera (Jacoby et al. 1998) at the Kitt Peak National Observatory 4-m telescope on UT February 7th and 8th, 2000. The wide field imager MOSAIC has eight 2k×4k thinned SITe CCDs. With $0.258''$ per pixel, it has a field of view of 36 arcmin on a side.

Our field was imaged through the $UBV\&I$ filters with integration times as shown in Table 2. The four nights were photometric. A detailed description of the data reduction and calibration of our survey is deferred to Bouché & Lowenthal (2003). To summarize, the images were bias-subtracted, corrected for the MOSAIC ghost pupil image, dome- and sky-flatfielded, cleaned for cosmic-rays, deprojected and registered onto a common frame, before being co-added. All magnitudes quoted below are measured in a $2 \times FWHM$ diameter aperture, where the FWHM is the seeing. The resulting magnitude limits are shown in Table 2.

From Monte-Carlo simulations, we estimated our completeness as a function of magnitude, and is shown in the inset of Fig. 1 as the dotted line. Our 50% completeness level is $m_I = 24.35$. Using the transformation

[3] Their study was aimed at investigating Lyα forest between $3.109 < z < 3.701$.

to convert our I-band magnitudes into AB magnitudes, i.e. $I_{\rm AB} = m_I + 0.47$, this corresponds to $I_{\rm AB} = 24.8$ ($\mathcal{R} \simeq \in\!\triangledown$) and to $\sim 0.6L^*$, where we used $m^*_{\mathcal{R}} = 24.5$ at $z \simeq 3$ (Steidel et al. 1999). In terms of L^*(today), it corresponds to $L/L^* \simeq 3$ using a distance modulus $m - M = 46.25 - 5\log h$ at $z = 3$ in our cosmology, $M^*_{g,\rm AB} - 5\log h = -20.04$ from SDSS (Blanton et al. 2001), and a $k-$correction between our I and the SDSS g filter of -0.30 (assuming the Irr SED of Coleman, Wu & Weedman 1980).

2.3. *Sample selection*

Sources were detected in the I-band using SExtractor (Bertin & Arnouts 1996), and aperture magnitudes were measured in all four bands using identical matched apertures defined in the I-band image to extract 30,000 objects with $I > 22.5$. Fig. 1 shows the position of each object in the $(U-B), (B-I)$ color space. We first selected a subset (1/3) of our I-band catalog using the color cuts shown by the dot-dashed lines in Fig. 1. This removes most of the $z \leq 1$ objects and reduces the amount of computing in the next step. We then estimated photometric redshifts of all objects in our subsample using the template fitting routine *Hyperz* from Bolzonella, Miralles & Pelló (2000) [4]. This constrains the redshift mainly via the shape of the SED at $\lambda_{rest} = 912$Å. In addition, we used the apparent magnitude as a redshift prior following the Bayesian prescription of Benítez (2000). The advantage of this last step is that it breaks most of the degenerancies of the SED fitting procedure (i.e. 4000Å break taken as a Lyα break) as shown by Benítez (2000). Finally, from our catalog now complemented with photometric redshifts $z_{\rm phot}$ and likelihood distributions $P(z)$, we selected galaxies with $22.5 < I < 24.35$ and computed the probability of each to be in three redshift slices of width $W_z = 0.15$: (1) $P_{\rm DLA} \equiv P(z_{\rm DLA} \pm 0.075)$, (2) $P_+ \equiv P([z_{\rm DLA} + 0.15] \pm 0.075)$, (3) $P_- \equiv P([z_{\rm DLA} - 0.15] \pm 0.075)$.

Out of 428 LBG candidates at redshift $2.75 < z < 3.25$, 84 objects with $P_{\rm DLA} > 0.5$ constitute our sample of candidates in a redshift slice centered on the DLA and are shown in Fig. 1 as open squares. This 0.5 threshold maximizes the number of objects and minimizes the likely outliers: $P_{outlier} \equiv P_z[|\Delta_z| > 0.2(1+z)] \leq 0.1$, following Benítez (2000). As a posteriori check, the distribution of LBG candidates in Fig. 1 shows that we are not excluding significant $z \sim 3$ objects in our color pre-selection. The number counts are shown in the inset of Fig. 1. Similarly 89 (17) LBG have $P_+ > 0.5$ ($P_- > 0.5$), respectively.

The slice width ($W_z = 0.15$) was chosen to correspond to the rms of the residuals between photometric and spectroscopic redshifts $\sigma(\Delta_z)$. $\sigma(\Delta_z)$ is $\simeq 0.15$ ($\sigma(\Delta z/(1+z)) \simeq 0.06$) in the redshift range $2.8 < z < 3.5$ from our analysis of photometric redshifts in the HDF-N. The residuals are similar to the accuracy in other studies (e.g. Fernandez-Soto et al. 2001). We defer the detailed description of our photometric redshift analysis to Bouché & Lowenthal (2003).

The slice width adopted here produces the largest sample in the smallest redshift slice. Our results are not affected when we chose a slice of half or twice the current size. At $z = 3$, the width $W_z = 0.15$ corresponds to ~ 100 Mpc (co-moving) or 25 Mpc (physical) assuming $h = 0.75$. Peculiar velocities of 7,500km s^{-1} would be required to have an effect on our results. This figure is much larger than any peculiar velocity in local clusters of galaxies. At $z = 3$, peculiar velocities are likely to be smaller than 1,000km s^{-1}. Therefore, peculiar velocities are not affecting our results.

3. RESULTS

3.1. *Clustering analysis*

Hierarchical models of galaxy formation predict that massive galaxies will likely be found in regions of high density, whereas low-mass galaxies are more uniformly distributed. This produces an enhancement of the clustering of high-mass galaxies since they tend to form near each other in rare overdense regions. Therefore, clustering is a probe of the mass distribution of galaxies. For instance, if LBGs cluster around DLAs, it would indicate that DLAs reside in massive dark halos.

A natural tool to investigate the clustering of galaxies is the two-point auto-correlation function $\xi_{gg}(r) = (r/r_o)^{-\gamma}$. However, our redshift accuracy $\sigma(\Delta_z) \simeq 0.15$ corresponds to $100h^{-1}$ Mpc. Therefore, without more accurate redshifts, the angular auto-correlation function $w_{gg}(\theta)$ is a more relevant statistic. Similarly to the two-point angular correlation function w_{gg}, the cross-correlation between DLAs and LBGs, ω_{dg}, gives the excess probability of finding an LBG in a small annulus of area $d\Omega$ between θ and $\theta + d\theta$ from a known DLA. The expected number of LBGs in that annulus is then:

$$N(LBG|DLA) = \overline{\Sigma}_g(1 + \omega_{dg}(\theta))d\Omega, \qquad (1)$$

where $\overline{\Sigma}_g$ is the underlying surface density of LBGs which is $\overline{\Sigma}_g = 0.041h^2$ Mpc^{-2} in our slice centered on the DLA. Thanks to the large field of view of the MOSAIC imager, there is little ambiguity in estimating the background surface density of LBGs. The background density is measured at $15 < r < 20h^{-1}$ Mpc, i.e. where galaxies are physically unrelated to the DLA.

Estimating w_{dg} accurately would require a large number of DLAs. Therefore, we investigated the spatial distribution of LBG candidates in two limiting cases: (i) assuming the LBG-DLA cross-correlation is the same as the LBG auto-correlation and (ii) assuming the cross-correlation is zero. In addition, we used a 3-D estimator of the cross-correlation. In the next two sections, we present our results and discussion of this analysis.

3.2. *Clustering results*

Figure 2 (left panels) shows the spatial distribution of LBG candidates in the three redshift slices, each of width $W_z = 0.15$: a) the slice at $z = z_{DLA} - 0.15$ with $P_- > 0.5$, b) the slice centered on the DLA at $z_{\rm DLA} = 2.974$, and c) the slice at $z = z_{\rm DLA} + 0.15$ with $P_+ > 0.5$. We smoothed the surface density with a Gaussian kernel of $2.5h^{-1}$ Mpc, shown with the contours in Fig. 2. The contours show the surface density $\delta = (\Sigma - <\Sigma>)/<\Sigma>$, where $<\Sigma>$ is the average surface density of the field. The thick contour shows $\delta = 0$, the continuous contours show $\delta = 1, 2, 3$, and the dotted contour shows $\delta = -1$.

[4] We note that we used the MOSAIC filter curves and the CCD response curves in performing the SED fits.

The right panels of Fig. 2 show the radial cumulative surface density centered on the DLA for the same three slices. The error bars are derived using bootstrap resampling method Mo, Jing & Boerner (1992).

The middle panels of Fig. 2 show that the surface density of LBG candidates is higher by a factor $\sim 3\times$ within $2.5-5$ Mpc than the averaged background galaxy density $\overline{\Sigma}_g$. This shows that at least some DLAs could reside in overdense regions. and implies a possible cross-correlation between this DLA and LBGs.

For the slice centered on the DLA, Fig. 2(b), we used the estimator of the cross-correlation proposed by Eisenstein (2002), which gives the volume average of the cross-correlation $< \overline{\xi}_{dg} >$. This estimator uses weightings that produce a spherically symmetric aperture rather than the cylindrical one used above. Fig. 3 shows $< \overline{\xi}_{dg} >$ as a function of the scale length of the Gaussian window. We find a 3-D overdensity $1+ < \overline{\xi}_{dg} >= n/\overline{n}_g \sim 4.97(\pm 2.99)$ using a Gaussian window of $5h^{-1}$ Mpc. The errors include the shot noise and the contribution of the clustering of the galaxies. We again conclude that this DLA seems to reside in an overdense region.

Next, in order to assess the significance of our result, we examined the two limiting situations presented and some possible sources of contamination.

In the first case, where we assume the LBG-DLA cross-correlation is the same as the LBG auto-correlation, i.e. $\xi_{dg} = \xi_{gg}$, we test whether this excess of galaxies around the absorber could be caused by the LBG clustering. A qualitative way to answer this is given by the dotted line in Fig 2, which shows the expected number of galaxies around the DLA due to the clustering of LBGs. That number is naturally found from Eq. 1 integrated from 0 to r_θ^{max} using the known auto-correlation of LBGs, ξ_{gg}, from Adelberger et al. (2003) converted into $\omega(\theta)$ using our redshift distribution. Clearly the angular clustering of LBGs alone cannot explain our data.

A more quantitative answer is given by computing the expected number of galaxies $N_{\rm exp}(r)$ again assuming $\xi_{dg} = \xi_{gg}$, and comparing it with the observed number of galaxies $N_{\rm obs}$. Table 3 shows the values for at various radii. E.g., within $2.5 < r_\theta < 5h^{-1}$ Mpc, we find 7 galaxies while 2.70 were expected. Could $N_{\rm obs}$ and $N_{\rm exp}$ be drawn from the same Poisson distribution of true mean $N_{\rm exp}$? The answer is given by testing the null hypothesis "$N_{\rm obs}$ and $N_{\rm exp}$ are drawn from the same Poisson distribution" versus "$N_{\rm obs}$ is greater than $N_{\rm exp}$", i.e. the observed overdensity is statistically significant. At $2.5 < r_\theta < 5h^{-1}$ Mpc, we find there is a probability of finding $\rm N_{obs} \geq 7$ galaxies (under the null hypothesis with $N_{\rm exp}$= 2.70) of $< 1\%$ (=P-value shown in Table 3). This implies the null hypothesis ought to be rejected, and the observed number of galaxies is *larger than* what one would expect from the LBG auto-correlation at the $> 99\%$ significance level.

In the second limiting case $\omega_{dg} = 0$, we test whether a purely random fluctuation in Σ could cause our result. This would decrease the expected number of galaxies slightly and therefore increase the significance level (see Table 3).

3.3. *Discussion*

Our results are not sensitive to the background density. The background density, itself, is a strong function of the magnitude limit and of the redshift slice width. A change of the background density Σ_g will change significantly both the observed and expected number of galaxies throughout the field. However, both are affected in the same way from Eq. 1 by Σ_g. The effect on the overdensity cancels out, since the overdensity is the excess of observed to the expected number of galaxies. The same relative overdensity by a factor of $\sim 3\times$ is observed with different magnitude cuts from 24 to 24.5, and with a width half or twice our current redshift width.

Alternative causes for the apparent excess of galaxies include contamination from low redshift sources (stars or galaxies) and signal from the cross-correlation between LBGs and other quasar absorption line clouds besides the DLA.

We estimate our contamination from low-redshift galaxies to be $\sim 10\%$ at $2.8 < z < 3.5$ based on our photometric redshift analysis in the HDF (Bouché & Lowenthal 2003). Another source of contamination is from faint stars with color similar to those of our LBG candidates. To estimate the stellar contamination, we used our star counts up to $m_I \leq 23.5$ and extrapolate them to our magnitude limit, assuming the counts to be constant at $m_I > 23.5$. This gives an upper limit on our stellar contamination of $< 7\%$. We note that both of these contaminations would dilute any clustering signal.

A high-resolution spectrum of this QSO (Ellison et al. 1999) shows there are 12 CIV metal-line systems with $3.1< z <3.5$ and 4 with $2.97< z <3.10$ (Tzanavaris 2002). However, the cross-correlation between CIV systems and LBGs is less strong ($r_o = 3h^{-1}$ Mpc) than the LBG auto-correlation ($r_o = 4h^{-1}$ Mpc, Adelberger et al. 2003). Therefore, on scales $5h^{-1}$ Mpc, the cross-correlation between CIV systems and LBGs cannot bias our results, for it would have to be larger than the LBG auto-correlation.

We close this section with a discussion of our search for the DLA itself. The QSO is not only lensed, but it also saturated the detector, thus preventing us from any attempt at PSF subtraction. Due to the brightness of the QSO, we are not sensitive to faint objects with impact parameters less than 5–6″. From our source catalog, we searched for all objects within 45″ (285 kpc in physical units) that have colors, i.e. photometric redshift, consistent with being at $z \sim 3$. We find one object at an impact parameter of $r_\theta = 145$ kpc (physical) that did not make it into our final catalogs for it is fainter than our completeness limit by 0.3mag. It has a magnitude of 24.65 ± 0.2 ($M_{I,\rm AB} = -21.35$) and a redshift $z_{\rm phot} = 3.03$. The colors of this galaxy are shown in Fig. 1 by the open triangle. Besides this galaxy, the closest object that did end up in our final catalog is 2.35 Mpc (co-moving) or 590 kpc (physical) away. We regard the galaxy 145 kpc away as an unlikely, but possible, candidate for the DLA.

4. SUMMARY AND CONCLUSIONS

To summarize, in the field of APM 08279+5255, we find 7 galaxies with $r_\theta < 4h^{-1}$ Mpc (186″) and within $|\Delta_z| = 0.075$, whereas one would expect 2.70 assuming that the cross-correlation is given by the LBG auto-correlation, i.e. that DLAs would be galaxies similar to

LBGs. The hypothesis that this is due to either the galaxy autocorrelation or to random fluctuation is rejected at the $> 95\%$ level. We estimated our contamination from stars or low-z galaxies to be $< 17\%$, since such contamination would only dilute our cross-correlation, so our results gives a lower limit on the cross-correlation.

We therefore conclude that, compared to the averaged background galaxy density $\overline{\Sigma}_g$, there is an overdensity $\Sigma/\Sigma_g \simeq 3$ of LBGs within $2.5 - 5$ Mpc around this $z_{\rm abs} = 2.974$ DLA. This scale corresponds to only 1.3 Mpc in physical coordinates at $z = 3$, when clusters would still be in formation and have core radii larger than 8 Mpc. Large scale structures at high redshifts shouldn't be unexpected. Recently, Shimasaku et al. (2003) reported the discovery of large-scale structure of Lyman alpha emitters at $z = 4.86$, $12h_{70}^{-1}$ Mpc (co-moving) in radius, based on wide-field imaging with Suprime-Cam on the Subaru telescope.

Our result implies a possible correlation between this DLA and LBGs, and that at least some DLAs reside in overdense regions. However, preliminary results in two of our other fields (Bouché & Lowenthal 2003) indicate a weak and an anti-correlation between LBGs and the other two DLAs. This could imply that not all DLAs reside in the same environment. This reinforces the idea that DLAs do not likely represent a single type of object, but are a wide variety of objects with high neutral hydrogen column density.

As a final note, the galaxy with the smallest impact parameter in our final slice centered on the DLA is $2.35h^{-1}$ Mpc (co-moving) or 590 kpc (physical) away from the QSO line of sight. In addition, we search for all objects within $45''$(285 kpc physical) and find an LBG candidate with $z_{\rm phot} = 3.03$ at $r_\theta = 145$ kpc, with a luminosity of $M_{I,\rm AB} = -21.35$. Due to the large impact parameter, this galaxy is unlikely to be responsible for the DLA, although it may be associated with it.

We are currently obtaining multi-object spectra with Gemini+GMOS of our LBG candidates within 5 h^{-1} Mpc of the QSO line-of-sight to investigate further the clustering of LBGs and the DLA.

NB acknowledges the support from the EARA Marie Curie Fellowship under contract HPMT-CT-2000-00132 and from the European Training Network 'The Physics of the Intergalactic Medium'. JDL acknowledges support from NSF grant AST-0206016. We thank M. Haehnelt, T. Theuns and J. Schaye for useful comments on an earlier draft. We thank A. Bunker and E. Gawiser for a careful reading of the manuscript, which improved the quality of the paper. Thanks to the Institute of Astronomy, where part of this work was accomplished.

REFERENCES

Adelberger, K. L., Steidel, C. C., Shapley A. E., & Pettini M. 2003, ApJ, 584, 45
Boissier, S., Péroux, C., & Pettini, M. 2003, MNRAS, 338, 131
Bouché, N., Lowenthal, J. D., Charlton, J. C., Bershady, M. A., Churchill, C. W., & Steidel, C. C. 2001, A&A550, 585
Bouché, N., & Lowenthal, J. D. 2003, in preparation
Bertin, E., & Arnouts, S. 1996, A&A, 117, 39
Benítez N. 2000, ApJ, 536, 571
Blanton, M. R., & SDSS collaboration 2001, AJ, 121, 2358
Bolzonella, M., Miralles, J-M., & Pelló, R. 2000, A&A, 363, 476
Coleman, G. D., Wu, C-C., & Weedman, D. W. 1980, ApJS, 43, 493
d'Odorico, V., Petitjean, P., & Cristiani, S. 2002, A&A, 390, 13
Eisenstein, D. J. 2002, preprint (astro-ph/0212084)
Ellison, S. L., Lewis, G. F., Pettini M., Chaffee, F. H., & Irwin, M. J. 1999, ApJ, 520, 456
Ellison, S. L., Pettini, M., Steidel, C. C., Shapley, A. E. 2001, ApJ, 549, 770
Francis, P. J., & Hewett, P. C. 1993, AJ, 105, 1633
Fernández-Soto, A., Lanzetta K.M., Chen H-W., Pascarelle S. M., & Yahata, N. 2001, ApJS, 135, 41
Fynbo, J. P. U., Møller, P., & Warren, S. J. 1999, MNRAS, 305, 849
Gawiser, E., Wolfe, A. M., Prochaska, J. X., Lanzetta, K. M., Yahata, N., & Quirrenbach, A. 2001, ApJ, 563, 628
Haehnelt, M. G., Steinmetz, M., & Rauch, M. 1998 ApJ, 495, 647
Irwin, M. J., Ibata, R. A., Lewis, G. F., & Totten, E. J., 1998, ApJ, 505, 529
Jacoby, G. H., Liang M., Vaughnn D., Reed R., & Armandroff, T. 1998, SPIE 3355, 721
Katz, N., Weinberg, D. H., Hernquist, L., & Miralda-Escudé, J. 1996, ApJ, 457, 57L
Khersonsky, V. K., & Turnshek, D. A. 1996, ApJ, 471, 657
Kobayashi, N., Terada, H., Goto, M., & Tokunaga, A. 2002, ApJ, 569, 676
Kulkarni, V. P., Hill, J. M., Schneider, G., Weymann, R. J., Storrie-Lombardi, L. J., Rieke, M. J., Thompson, R. I., & Jannuzi, B. T. 2000, ApJ, 536, 36
Le Brun, V., Bergeron, J., Boissé, P., & Deharveng, J. M. 1997, A&A, 321, 733
Lewis G. F., Robb R. M., & Ibata R. A. 1999, PASP, 111, 1503
Lowenthal, J. D., Hogan, C. J., Green, R. F., Woodgate, B. E., Caulet, A., Brown, L., & Bechtold, J. 1995, ApJ, 451, 484
Maller, A. H., Prochaska, J. X., Sommerville, R. S., & Primack, J. R. 2000, in *Clustering at high redshift*, ASP vol. 200, Eds A. Mazure
Mo, H. J., Jing, Y. P., & Boerner, G. 1992, ApJ, 392, 452
McDonald, P., & Miralda-Escudé, J. 1999, ApJ, 519, 486
Petitjean, P., Aracil, B., Srianand, R., & Ibata, R. A. 2000, A&A, 359, 457
Pettini, M., Ellison, S. L., Steidel, C.C., & Bowen, D. 1999, ApJ, 510, 576
Pettini, M., Ellison, S. L., Steidel, C.C., Shapley, A. E., & Bowen, D.V. 2000, ApJ, 532, 65
Prochaska, J. X., & Wolfe, A. M. 202, ApJ, 566, 68
Prochaska, J. X., & Wolfe, A. M. 1997, ApJ, 487, 73
Rao, S. M., & Turnshek, D. A. 2000, ApJS, 130, 1
Schlegel, D., Finkbeiner, D., & Davis, M., ApJ, 1998, 500, 525
Shimasaku, K., & Subaru team 2003, ApJ, accepted (preprint astro-ph/0302466)
Steidel, C. C., & Dickinson, M. 1992, ApJ, 394, 81
Steidel, C. C., & Hamilton, D. 1992, ApJ, 104, 941
Steidel, C. C., & Hamilton, D. 1993, ApJ, 105, 2017
Steidel, C. C., Dickinson, M., Meyer D., Adelberger, K. L., & Sembach, K. R. 1997, ApJ, 480, 568
Steidel ,C. C., Adelberger, K. L., Giavalisco, M., Dickinson, M., & Pettini, M. 1999, ApJ, 519, 1
Tzanavaris, P., & Carswell, R. F. 2003, MNRAS, submitted (astro-ph/0212393)
Tzanavaris, P. 2002, Ph.D. Thesis, University of Cambridge
Wolfe, A. M., Turnshek, D. A., Smith, H. E., & Cohen, R. D. 1986, ApJS, 61, 249
Wolfe, A. M. 1993, ApJ, 402, 411
Wolfe, A. M., Lanzetta, K. M., Foltz, C. B., & Chaffee, F.H. 1995, ApJ, 454, 698

TABLE 1
PROPERTIES OF THE FIELD.

Parameter	Value
QSO APM 08279+5255 ($z_{\rm em} = 3.91$)	
R.A. (J2000)	$08^h31^m41.6^s$
Decl. (J2000)	$52°45'17''$
m_R (mag) ...	15.2
A_U[a](mag) ...	0.20
E_{B-V}[a](mag) .	0.04
Damped Ly-α Cloud ($z_{\rm abs} = 2.974$)	
$\log N_{HI}$[b].....	$19.8 - 20.3$
$[Fe/H]$[b].....	-2.31

References. — (a) from Schlegel et al. (1998), averaged over the field; (b) Petitjean et al. (2000)

TABLE 2
SUMMARY OF OBSERVATIONS.

Filter	Exp. /Frames (sec./#)	Airmass (min-max)	FWHM (arcsec)	$\mu_I(1\sigma)$ (m_{AB}/arcsec^2)	$m_I(3\sigma)$ [1] (m_{AB})	Completeness 50% [1] (m_{AB})
U	13500/15	1.07-1.17	1.1	28.61	26.68	
B	2100/7	1.14-1.27	1.1	28.37	26.42	
V	3000/10	1.21-1.37	1.2	28.23	26.19	
I	7590/20	1.11-1.62	1.1	27.62	25.68	24.80

[1]measured inside a 2× FWHM diameter aperture.

TABLE 3
NULL HYPOTHESIS TEST AT VARIOUS RADII.

r_θ (h^{-1} Mpc)	Σ (h^2 Mpc^{-2})	$N_{\rm obs}$[a]	$N_{\rm exp}$[b]	P-value[c]
$0 - 2.5$.....	0.05	1	1.04	0.27 (0.19)
$2.5 - 5$.....	0.12	7	2.70	<0.01 (<0.01)
$5 - 10$.....	0.07	15	9.90	0.10 (0.07)
$15 - 20$	0.04	16	16.71	0.50 (0.43)

[a]Observed number of neighbors.

[b]Expected number of neighbors assuming $\xi_{dg} = \xi_{gg}$.

[c]P-values of the null hypothesis, i.e. probability that $N_{\rm obs}$>$N_{\rm exp}$ if $N_{\rm obs}$ were drawn from a distribution of true mean equal to $N_{\rm exp}$, assuming $\xi_{dg} = \xi_{gg}$ (assuming $\omega_{dg} = 0$).

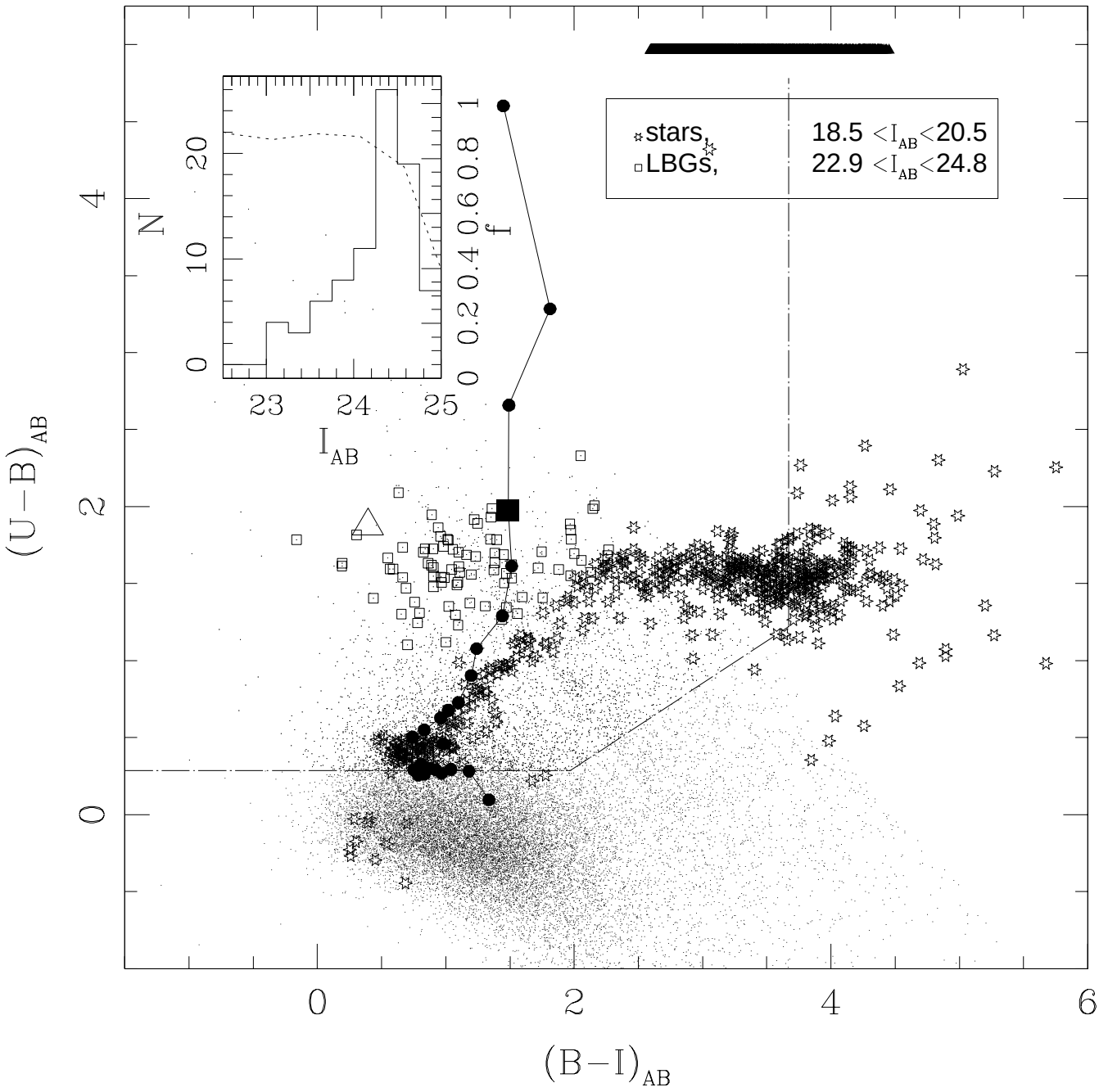

FIG. 1.— Color-color $(U-B)_{AB}$, $(B-I)_{AB}$ diagram. Each dot represents one of our $\sim 30,000$ objects in our image with $23.0 < I_{AB} < 24.80$. Open squares are our LBGs candidates in the redshift slice centered on the DLA ($z_{abs} = 2.974$), i.e. with $P_{\rm DLA} > 0.5$ (see text). Objects with U and B upper limits (filled triangles) have their $U-B$ set to an arbitrary constant ($= 5$), and the B magnitude limit is used in $B-I$. Stars show the locus of stellar objects with $18.5 < I_{AB} < 20.5$. The open triangle is the closest LBG to the line of sight, which has an impact parameter of 145 kpc (see § discussion). The evolutionary track of an Irr SED (averaged over different dust content, from $A_v = 0$ to $A_v = 1.2$) is shown in redshift steps of 0.1 for illustrative purposes; the $z = 3$ mark is shown with the large filled square. We pre-selected objects within the color cut shown with the dot-dashed lines. The inset shows their number counts (N) as a function of magnitude (I_{AB}). The dotted line shows our completeness (f).

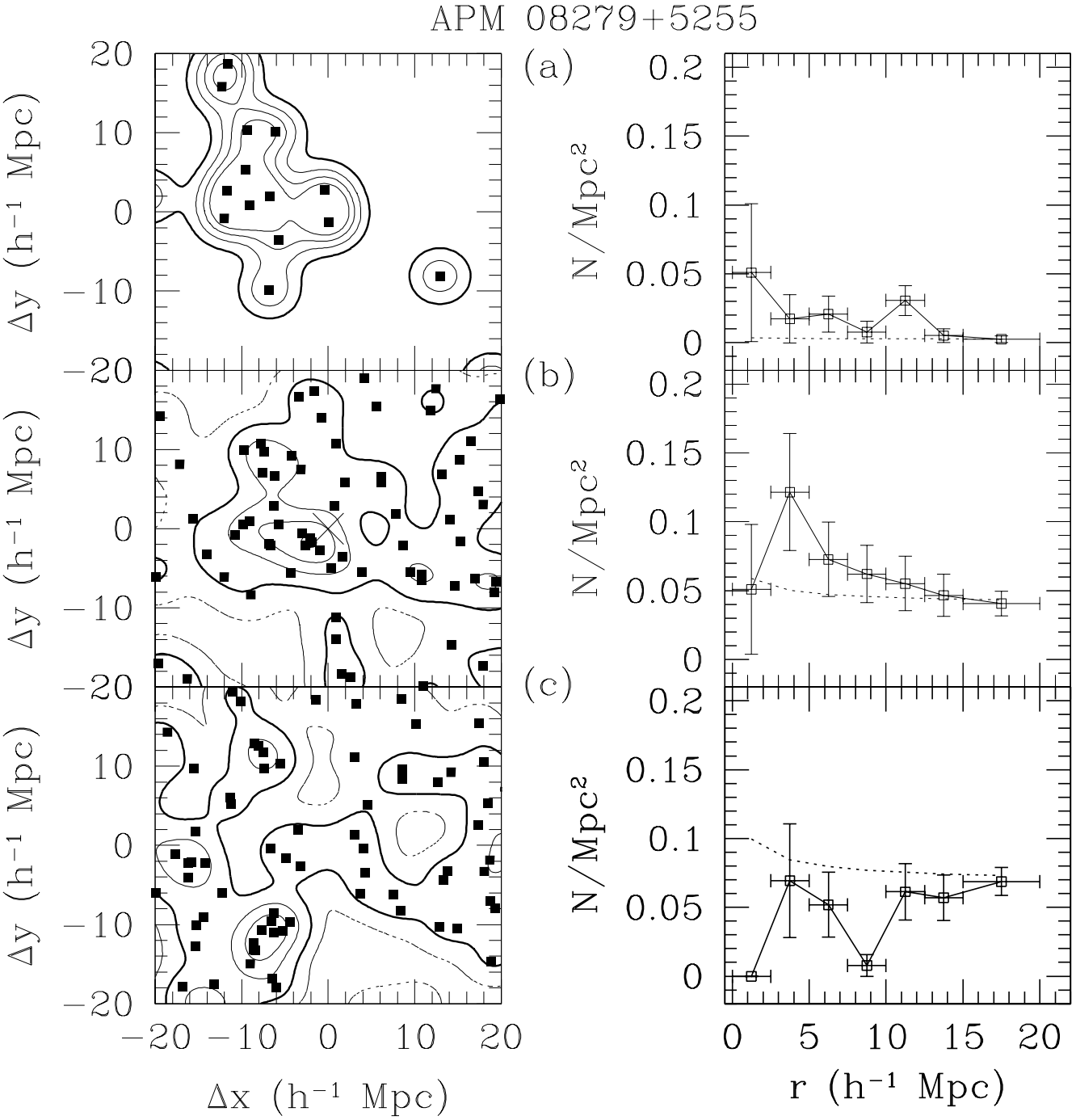

FIG. 2.— The spatial distribution of LBG candidates (left) and the radial surface distribution (right) for three different redshift slices: a) slice centered at $z = z_{DLA} + 0.15$, with $P_+ > 0.5$; b) slice centered at $z = z_{DLA}$, with $P_{\rm DLA} > 0.5$; and c) slice centered at $z = z_{DLA} - 0.15$, with $P_- > 0.5$. Panel b) is centered on the DLA, marked by the cross. Panels a) and c) shows the distribution of galaxies unrelated to the DLA. Contours on the left panels shows the surface densities $\delta = \Sigma/\overline{\Sigma} - 1$, where $\overline{\Sigma}$ is the mean density over the entire field. The thick contour shows $\delta = 0$; the continous contours show $\delta = 1, 2, 3$; the dotted countours show $\delta = -1$. The error bars on the right panels are computed using bootstrap resampling. The QSO line-of-sight is maked with a cross. For galaxies within the slice centered on the DLA (b), the surface density distribution shows a peak (significant at $> 95\%$; see text) at ~ 4 Mpc from the DLA. This indicates an over-density of galaxies by a factor $\sim 3\times$ on scales $2.5 - 5$ Mpc from the DLA compared to the averaged background galaxy density $\overline{\Sigma}_g$.

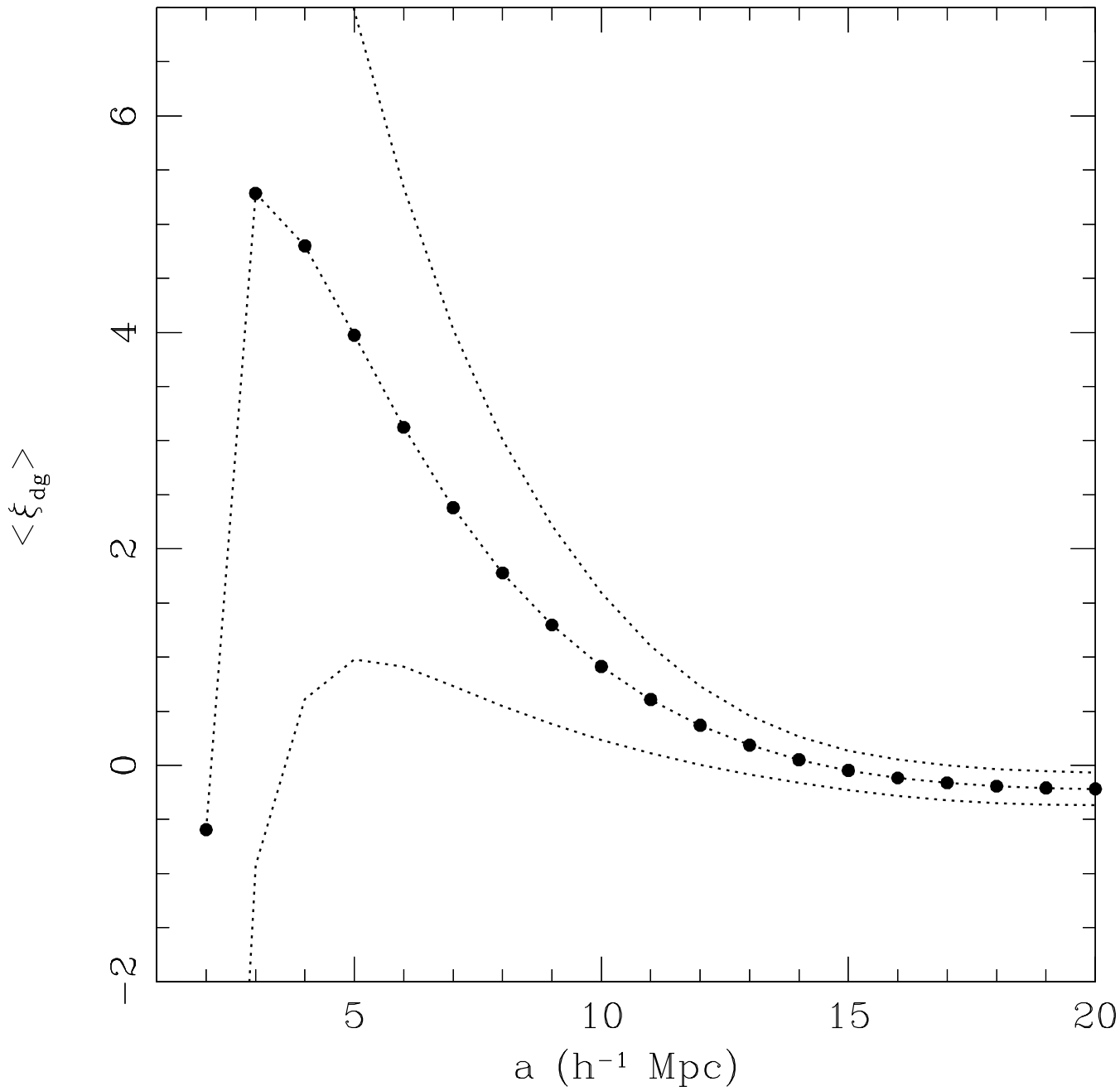

FIG. 3.— The volume averaged (using a Gaussian window function) of the cross-correlation function ξ_{dg} , following Eisenstein (2002) is shown as a function of the scale length a of the window function. The (1σ) errors, shown as the dotted lines, include the Poission variance and the variance from the clustering of the galaxies.